

Artificial Atoms: The Superconducting (transmon) Qubit

Georgios Vougioukas, AM:2016039002

I. INTRODUCTION

The project aimed at the understanding of how artificial atoms can be used as quantum computational units (qubits) [1]. Conventionally, atoms are utilized as qubits due to their inherent quantum mechanical behaviour (and interactions with each other), In contrast, appropriately designed superconducting circuits (“artificial atoms”, quantum LC oscillators) can display the necessary quantum mechanical behaviour and thus be utilized as qubits.

Mathematically, a superconducting LC circuit can be described as a quantum harmonic oscillator (QHO). It can be shown that the QHO offers an infinite “ladder” of discrete energy levels. Considering only the two lower energy levels of the aforementioned ladder, QHO can be effectively seen as a qubit. The lower energy levels are chosen due to the fact that the system will naturally, given sufficient time, end up in its lowest energy state. That way initialisation can be easily performed. Utilizing superconducting (dissipationless) LC circuits as QHOs, allows for controlling the state of a qubit using microwave photons; qubit control is performed using “radio” equipment like waveform and RF generators. Qubit-qubit interactions can be mediated by controlling the resonance frequency of each of the involved (in the interaction) qubits.

II. QHO BASICS

A simple example of a (classical) harmonic oscillator, is the mass attached to a spring system (Fig. 1-left). The (linear) restoring force of the spring offers a quadratic potential energy term of the form:

$$U(x) = \frac{1}{2}kx^2, \quad (1)$$

where x is the displacement from the resting position and k the spring’s constant. The total energy of the system comprises of the sum of the kinetic energy term and the aforementioned potential term. The Hamiltonian can be then expressed as:

$$H = \frac{1}{2}mu^2 + \frac{1}{2}kx^2 = \frac{p^2}{2m} + \frac{kx^2}{2}, \quad (2)$$

where u is the speed of the mass (m) and p its momentum.

By replacing the variables with their respective operators [2], the classical Hamiltonian can be used to describe the energy of quantum harmonic oscillators:

$$\hat{H} = \frac{\hat{p}^2}{2m} + \frac{k\hat{x}^2}{2} = \frac{\hat{p}^2}{2m} + m\omega_q^2 \frac{\hat{x}^2}{2}, \quad (3)$$

where $\omega_q = \sqrt{k/m}$ is the resonance frequency of the oscillator. \hat{p} , \hat{x} are the momentum and position operators, respectively, defined by their action in a wave function as:

$$\hat{p}|\psi(x)\rangle = -j\hbar \frac{\partial}{\partial x} \psi(x), \quad (4)$$

$$\hat{x}|\psi(x)\rangle = x\psi(x). \quad (5)$$

While not explicitly shown, the state is also a function of time (it evolves). The last, justifies the use of partial derivative in the definition of the action of \hat{p} .



Fig. 1: Examples of systems that can be mathematically described as simple harmonic oscillators, a mass attached to a spring (right) and an LC oscillator (left).

With the Hamiltonian available, the energy levels/eigenvalues of the Hamiltonian can be evaluated by solving the time-independent Schrödinger equation:

$$\hat{H} |\psi_E(x)\rangle = E |\psi_E(x)\rangle. \quad (6)$$

To solve Eq. (6) and acquire the eigenvalues and respective eigenfunctions, one can either work Eq. (6) from a differential equation perspective, or can use commutator and operator algebra. Following the algebra path, the following operators are defined:

$$\begin{aligned} \alpha^- &= \sqrt{\frac{m\omega_q}{2\hbar}} \left(\hat{x} + j \frac{\hat{p}}{m\omega_q} \right), \\ \alpha^+ &= \sqrt{\frac{m\omega_q}{2\hbar}} \left(\hat{x} - j \frac{\hat{p}}{m\omega_q} \right). \end{aligned} \quad (7)$$

That way:

$$\begin{aligned} \alpha^+ \alpha^- &= \frac{m\omega_q}{2\hbar} \left(\hat{x} - j \frac{\hat{p}}{m\omega_q} \right) \left(\hat{x} + j \frac{\hat{p}}{m\omega_q} \right) = \frac{m\omega_q}{2\hbar} \left(\hat{x}^2 + j \frac{\hat{x}\hat{p}}{m\omega_q} - j \frac{\hat{p}\hat{x}}{m\omega_q} + \frac{\hat{p}^2}{m^2\omega_q^2} \right) \\ &= \frac{m\omega_q}{2\hbar} \left(\hat{x}^2 + j \frac{1}{m\omega_q} (\hat{x}\hat{p} - \hat{p}\hat{x}) + \frac{\hat{p}^2}{m^2\omega_q^2} \right) = \frac{m\omega_q}{2\hbar} \left(\hat{x}^2 + j \frac{1}{m\omega_q} [\hat{x}, \hat{p}] + \frac{\hat{p}^2}{m^2\omega_q^2} \right) \\ &= \frac{m\omega_q}{2\hbar} \left(\hat{x}^2 - \frac{\hbar}{m\omega_q} + \frac{\hat{p}^2}{m^2\omega_q^2} \right) = \frac{m\omega_q \hat{x}^2}{2\hbar} + \frac{\hat{p}^2}{2\hbar m\omega_q} - \frac{1}{2}. \end{aligned} \quad (8)$$

Thus, $\hat{H} = \hbar\omega_q (\alpha^+ \alpha^- + 1/2)$. In Eq. (8), the fact that $[\hat{x}, \hat{p}] = j\hbar$ was used:

$$\begin{aligned} (\hat{x}\hat{p} - \hat{p}\hat{x}) \psi(x) &= j\hbar \left(\frac{\partial}{\partial x} x \psi(x) - x \frac{\partial}{\partial x} \psi(x) \right) \stackrel{(1)}{=} j\hbar \left(\psi(x) + x \frac{\partial}{\partial x} \psi(x) - x \frac{\partial}{\partial x} \psi(x) \right) \\ &= j\hbar \psi(x), \end{aligned} \quad (9)$$

where in point (1) the product rule was used. The impact of the operators on the state is given as:

$$\begin{aligned} \hat{x}\hat{p} |\psi(x)\rangle &= -j\hbar x \frac{\partial}{\partial x} \psi(x), \\ \hat{p}\hat{x} |\psi(x)\rangle &= -j\hbar \frac{\partial}{\partial x} x \psi(x). \end{aligned} \quad (10)$$

Defining the operator $\hat{N} = \alpha^+ \alpha^-$, with $\hat{N} |n\rangle = n |n\rangle$, the Hamiltonian becomes:

$$\hat{H} = \hbar\omega_q \left(\hat{N} + 1/2 \right). \quad (11)$$

It can be easily shown [2] that the following commutator relationships hold:

$$\begin{aligned} [\alpha^-, \alpha^+] &= 1, \\ [\alpha^-, \hat{N}] &= \alpha^-, \\ [\alpha^+, \hat{N}] &= -\alpha^+. \end{aligned} \quad (12)$$

To find \widehat{N} 's eigenvalues, the aforementioned commutators will be used. First, a new vector (instead of $|n\rangle$) is considered, namely $\alpha^+ |n\rangle$. Then, \widehat{N} acts on the newly defined vector and the operation can be expressed as:

$$\widehat{N}(\alpha^+ |n\rangle) = [\alpha^+ \widehat{N} - \alpha^+ \widehat{N} + \widehat{N} \alpha^+] |n\rangle = [\alpha^+ \widehat{N} - (\alpha^+ \widehat{N} - \widehat{N} \alpha^+)] |n\rangle. \quad (13)$$

The term within the parenthesis is the commutator $[\alpha^+, \widehat{N}]$ (See Eq. (12)). Thus, utilizing the fact that $\widehat{N} |n\rangle = n |n\rangle$, Eq. (13) becomes:

$$\widehat{N}(\alpha^+ |n\rangle) = [\alpha^+ \widehat{N} + \alpha^+] |n\rangle = \alpha^+ (\widehat{N} + 1) |n\rangle = (n + 1) \alpha^+ |n\rangle. \quad (14)$$

Eq. (14) demonstrates that given an eigenvector $|n\rangle$ (with respective eigenvalue n), the vector $\alpha^+ |n\rangle$ is another eigenvector of \widehat{N} with an eigenvalue of $n + 1$. It can be similarly shown that $\alpha^- |n\rangle$ displays the same behaviour with an eigenvalue of $n - 1$.

The aforementioned results show that \widehat{N} has an infinite number of eigenstates and by extension, \widehat{H} has an infinite number of energy levels:¹

$$E_n = \hbar\omega_q (n + 1/2), n \in \mathbb{N}_0. \quad (15)$$

III. THE QUANTUM LC OSCILLATOR

A. Conventional (quantum) LC Oscillator

As stated in Sec.II, the harmonic oscillator framework can be used to describe a number of systems. Besides the mass-spring system, the energy of an LC circuit can be mathematically described using Eq. (2), by simply replacing the momentum term (p) with the charge at the circuit's capacitor (Q) and the displacement (x) term, by the magnetic flux (Φ) of the circuit's inductor:²

$$H = \frac{1}{2}CV^2 + \frac{1}{2}LI^2 = \frac{Q^2}{2C} + \frac{\Phi^2}{2L}, \quad (16)$$

where C is the capacitance and L the inductance. V is the voltage at the capacitor's terminals and I the current in the circuit. The resonance frequency of the system is given by $\omega_q = \sqrt{\frac{1}{LC}}$.

The system can be quantized by directly replacing the variables with their respective operators [3]:

$$\widehat{H} = \frac{\widehat{Q}^2}{2C} + \frac{\widehat{\Phi}^2}{2L}, \quad (17)$$

where \widehat{Q} the charge operator and $\widehat{\Phi}$ the flux operator with $[\widehat{\Phi}, \widehat{Q}] = j\hbar$.

As stated earlier, to exploit the quantum mechanical behaviour offered by an LC oscillator, the circuit must be cooled down to temperatures in the order of mK. That way, appropriate metals can be used in their superconducting state. In normal operating conditions (temperatures), electrical resistance is manifested as the electrons scatter in the crystal lattice of the metal. Such scattering events are due to lattice vibrations or crystal impurities. At superconducting-level temperatures, those vibrations effectively "slow down" and allow for current to flow through the superconductor. Although vibrations still exist, they lead to the formation of electron pairs (referred to as Cooper pairs), which "slip" through the lattice leading to a dissipationless current flow (the carriers are the pairs).

Having stated the above, the charge can be defined as the number of Cooper pairs present in the area of interest. The aforementioned statement can be seen as the eigenvalue perspective of the operator definition

¹It is assumed that $\alpha^- |0\rangle = 0$.

²Although it is more intuitive to match the position to the charge and the momentum to the flux, the non-linearity that will be subsequently introduced to the "magnetic" part of the circuit, would result a nonlinear kinetic energy term (it is "clearer" to work with a nonlinear potential term).

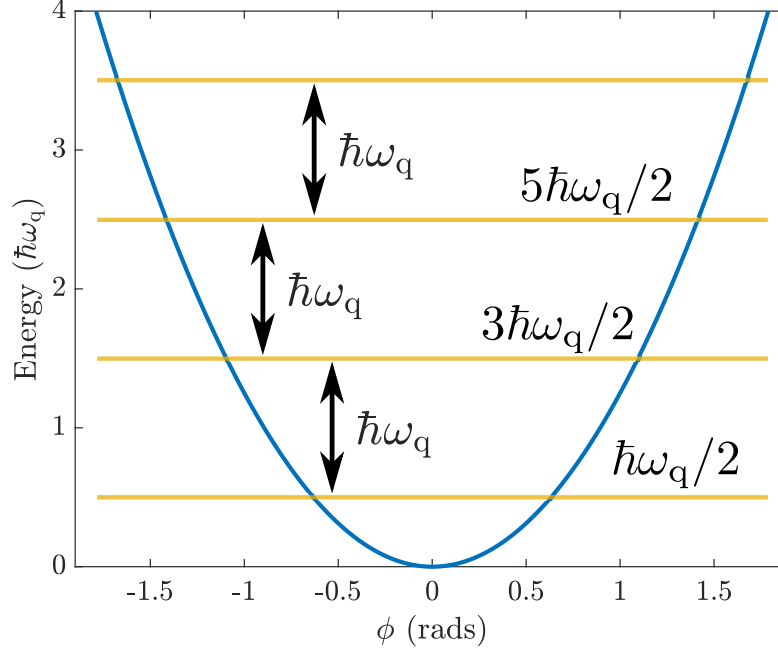


Fig. 2: Potential energy (potential term in Eq. (18)) of a (quantum) LC oscillator. Using Eq. (15), the energy levels are also shown. It was assumed that $F_q = \frac{\omega_q}{2\pi} = 5$ GHz and $E_L = 50E_c$.

$\hat{Q} = 2e\hat{n}$. Similarly, the flux operator can be defined using the flux quantum $\Phi_0 = h/2e$, as $\hat{\Phi} = \phi_0\hat{\phi}$, where $\phi_0 = \Phi_0/2\pi$ is the reduced flux quantum [3]. Thus, the Hamiltonian of Eq. (17) can be rewritten as:

$$\hat{H} = 4E_c\hat{n}^2 + \frac{1}{2}E_L\hat{\phi}^2, \quad (18)$$

where $E_c = e^2/2C$ which can be seen as the energy required to place each electron of a Cooper pair to the capacitor of the circuit, while $E_L = \phi_0^2/L$. The resonance frequency can be given as $\omega_q = \sqrt{8E_cE_L}/\hbar = \sqrt{1/LC}$. The energy levels/eigenvalues of the Hamiltonian in Eq. (18) are given by Eq. (15).

The potential energy of the quantum LC oscillator is given in Fig. 2. The first obstacle towards using a quantum LC oscillator as a qubit can be seen at that plot. The energy levels are equidistant. Given sufficient time, the system will “relax” at its ground state ($\hbar\omega_q/2$). Assuming that only the two lowest energy levels were to be exploited, if a photon of energy $\hbar\omega_q$ was to be used to excite the system to the second energy level, due to the equidistant energy spacing, it would not be possible to be “sure” for the state the system was excited at. Thus, the harmonicity of the LC oscillator must be “destroyed” and that can be achieved by introducing nonlinearity in the circuit.

Fig. 2, shows another way of looking at the requirement for ultra-low temperatures. Assume that nonlinearity was introduced in the circuit (as will be shown in the next section) and the two lowest energy levels were used to realize a quantum two level system, a qubit. It is further assumed that the said qubit is initialized at its ground state and $\omega_q = 2\pi \cdot (5$ GHz). The system will be excited if energy of $E_q = \hbar F_q$ is offered. The amount of energy can be offered by a photon of frequency F_q but it can also be offered if the system is placed at an environment of temperature $T_q = \hbar F_q/k_B \approx 0.2$ K, where k_B the Boltzmann’s constant. Temperatures greater than T_q can also excite the system at higher energy levels.

B. Quantum (L)C Oscillator with Josephson Junction

In order for the harmonicity exhibited by the LC oscillator to break, a nonlinearity will be introduced in the form of a nonlinear element. The said element is the Josephson junction (Fig. 3) [4]. On a higher

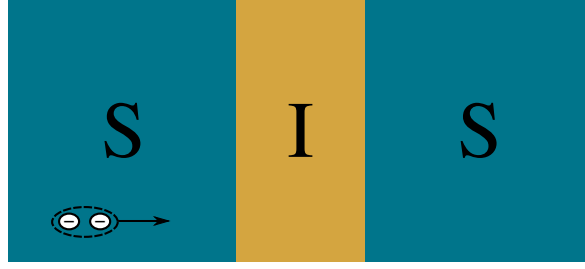


Fig. 3: The Josephson junction, a nonlinear element comprised of two superconductors separated by a thin insulating layer. Cooper pairs tunnel through the junction and as a result current flows without applying a voltage at the terminals. The element can be treated as a nonlinear inductor.

level, the phase difference between the wave functions³ at either end of the junction causes a flow of current in the form of [4]:

$$I = I_c \sin(\delta), \quad (19)$$

where I_c is the critical current of the junction, above which the current flow is dissipative and δ is the aforementioned phase difference. The phase difference δ , is connected to the applied voltage V (at the terminals of the junction) as:

$$\delta(t) = \delta(0) + \frac{2e}{\hbar} \int V(t) dt, \quad V(t) = \frac{\hbar}{2e} \frac{d\delta}{dt}. \quad (20)$$

Eq. (19) in conjunction with Eq. (20) show that even if $V(t) = 0$ (zero voltage across the junction) current flows. On the other hand, if a DC bias is applied, then, according to the equations, the current exhibits a sinusoidal oscillation. However, due to the presence of \hbar (and e) terms which are really small numbers (compared to values that $V(t)$ would attain), the frequency of oscillations is extremely high. Thus, the movement of the pairs can be thought as highly constrained and thus “no” net current flow is offered.

The behaviour of the Josephson junction can be further demonstrated by using the voltage and current relationships of Eq. (19) and Eq. (20):

$$\frac{\partial I}{\partial t} = \frac{\partial I}{\partial \delta} \frac{\partial \delta}{\partial t} = I_c \cos(\delta) \frac{2e}{\hbar} V(t) \Leftrightarrow V(t) = \frac{\hbar}{2e I_c \cos(\delta)} \frac{\partial I}{\partial t} = L_J(\delta) \frac{\partial I}{\partial t}. \quad (21)$$

Thus, the Josephson junction can be seen as an Inductor exhibiting nonlinear inductance. It can be shown that phase difference δ is associated with the notion of generalized flux [3]. Thus, the inductance (and the rest of the relationships involving δ) can be expressed as:

$$L_J(\Phi) = \frac{\Phi_0}{2\pi I_c} \frac{1}{\cos(2\pi\Phi/\Phi_0)}. \quad (22)$$

By integrating the product IV over given time periods, the energy stored in a Josephson junction can be calculated. Then, the Hamiltonian of an oscillator utilizing a Josephson junction instead of a conventional inductor is given as:

$$\hat{H} = 4E_c \hat{n}^2 - E_J \cos(\hat{\phi}), \quad (23)$$

where $E_J = I_c \phi_0$ is the energy “stored” in the junction, in the form of the movement of the pairs (current flow). E_c is defined as in Eq. (18) with a capacitance $C_{\text{tot}} = C_J + C_S$, where C_J is the inherent capacitance of the junction and C_S any additional shunt capacitance. The cosinusoidal term involving the flux can be expanded to a power series, where the first quadratic term resembles the effect of a linear inductor.

³The Cooper pairs at each side of the junction share the same wave function [4].

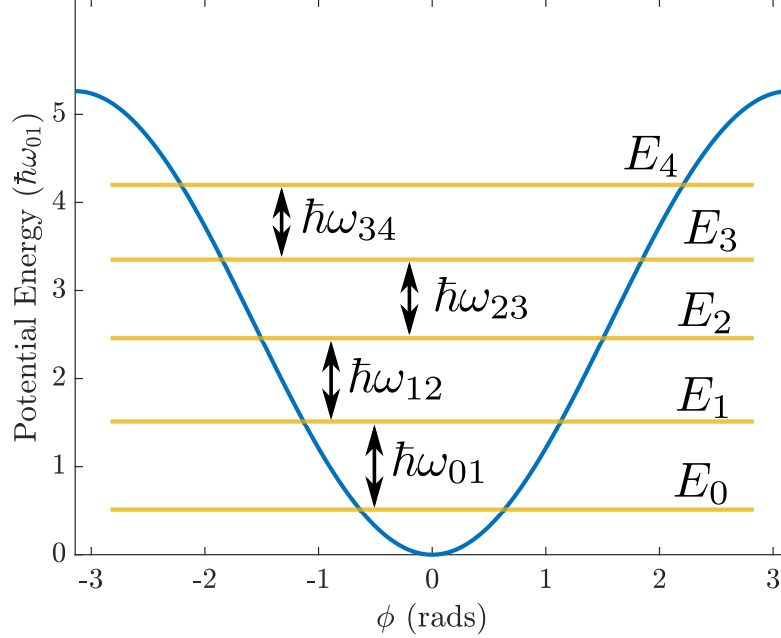


Fig. 4: Potential energy of an LC oscillator equipped with a Josephson junction (instead of a conventional inductor). Using Eq. (24), the energy levels are also shown. The potential plotted is $E_J - E_J \cos(\phi)$. It was assumed that $F_q = \frac{\epsilon_q}{2\pi} = 5$ GHz and $E_J = 50E_c$.

The energy levels of the system can be found in a way similar to Sec. II [5]:

$$E_n \simeq -E_J + \sqrt{8E_c E_J} \left(n + \frac{1}{2} \right) - \frac{E_c}{12} (6 * n^2 + 6 * n + 3). \quad (24)$$

It is evident from Eq. (24), that the energy spectrum is no longer harmonic (i.e., the spacing between energy levels is not the same). Eq. (24) is valid for the first few levels n and assuming $E_J \gg E_c$, i.e., operation in the *transmon* regime. Based on Eq. (24), the energy separation between the two lowest energy levels can be given by:

$$\omega_{01} = (E_1 - E_0) / \hbar \simeq \left(\sqrt{8E_c E_J} - E_c \right) / \hbar. \quad (25)$$

The potential energy of the quantum oscillator with a Josephson junction is given in Fig. 4. The anharmonicity is evident and thus, excitations between energy levels can be individually “addressed”, utilizing photons of the appropriate energy; by limiting all the operations to the lowest two energy levels, a qubit can be realized.

As stated in the previous paragraphs, operation in the transmon regime is assumed, where $E_J \gg E_c$. In that case, the energy levels are less sensitive to charge noise, however, the greater the ratio E_J/E_c is, the larger the harmonicity in the energy spectrum [5], [6]. Controlling the value of the shunt capacitance C_s , effectively controls E_c and thus, the ratio E_J/E_c can be controlled.

IV. SINGLE QUBIT GATES

In Fig. 5, a simplified setup is shown for the control of a superconducting qubit. The driving circuitry is coupled to the qubit via capacitor C_d . Assuming a conventional inductor model, it can be shown that

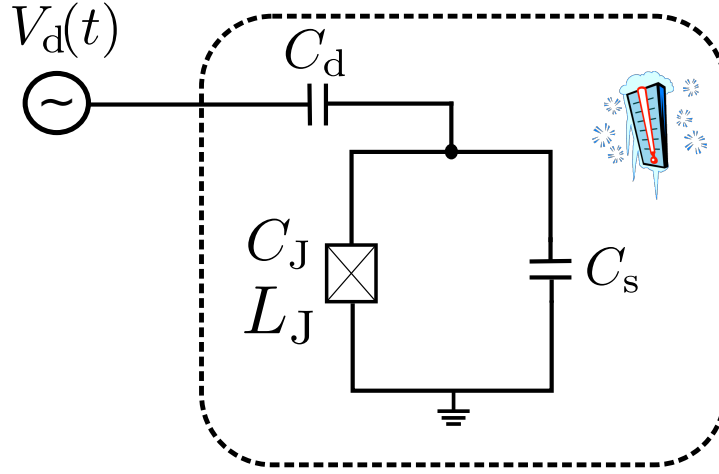


Fig. 5: Realizing single qubit gates. Excitation of the qubit is performed using microwave photons.

the Hamiltonian of the system (assuming weak coupling) is:⁴

$$\hat{H} = \frac{\hat{Q}^2}{2C} + \frac{\hat{\Phi}^2}{2L_J} + \frac{C_d}{C_{\text{tot}}} V_d(t) \hat{Q}. \quad (26)$$

A simple derivation (up to a sign) for the extra (interaction) energy term would be to consider $E_d = \frac{1}{2} C_d (V_d(t) - V_q)^2$ and keeping only the terms involving both the drive and the qubit.

Using the α^\pm operators defined in Sec. II, the charge operator can be expressed as (in a direct analogy with the mechanical oscillator):

$$\hat{Q} = -j\sqrt{\frac{\hbar}{2Z}} (\alpha^- - \alpha^+), \quad (27)$$

where $Z = \sqrt{L/C}$. That way, the Hamiltonian of the driven system becomes:

$$\hat{H} = \hbar\omega_{01} (\alpha^+ \alpha^- + 1/2) - \frac{C_d}{C_\Sigma} V_d(t) j\sqrt{\frac{\hbar}{2Z}} (\alpha^- - \alpha^+). \quad (28)$$

Assuming that the system is limited to the (two) lowest energy levels, the first term of the above Hamiltonian can be written as:

$$\hat{H}_{\text{LC}} = -\frac{1}{2} \hbar\omega_{01} \sigma_z, \quad (29)$$

where the eigenvalues of \hat{H}_{LC} correspond to the energy levels around the level $(E_0 + E_1)/2$. The sign defines which energy level corresponds to which computational basis state (i.e., $|0\rangle, |1\rangle \Rightarrow E_{0,1/1,0}$). Describing the oscillator as a two level system allows for mapping the operators α^\pm to the raising and lowering matrices σ^\pm . Thus, the Hamiltonian of Eq. (28) becomes:

$$\hat{H} = -\frac{1}{2} \hbar\omega_{01} \sigma_z + \Omega V_d(t) \sigma_y, \quad (30)$$

where $\Omega = \frac{C_d}{C_\Sigma} \sqrt{\frac{\hbar}{2Z}}$. The Hamiltonian is time-dependent. Thus, as shown in the course, a rotating frame should aid in solving the Schrödinger's equation. The first term of the Hamiltonian causes a precession

⁴The driving capacitor C_d is appropriately chosen so as to minimize the energy loss from the qubit to the external environment (i.e., losses towards the generator).

around the z axis at ω_{01} . Assuming a new reference frame, rotating at ω_{01} , the driving Hamiltonian (in that frame) can be expressed as:

$$\tilde{H}_d = \Omega V_d(t) (\cos(\omega_{01}t) \sigma_y - \sin(\omega_{01}t) \sigma_x). \quad (31)$$

The driving voltage can be given as:

$$V_d(t) = s(t) \sin(\omega_d t + \phi) = s(t) (I \sin(\omega_d t) + Q \cos(\omega_d t)), \quad (32)$$

where $I = \cos(\phi)$ and $Q = \sin(\phi)$. It has to be noted that ϕ refers to the phase of the driving signal and is not related (in this context) to the flux. That way, the driving Hamiltonian in the rotating frame becomes:

$$\tilde{H}_d = \frac{1}{2} \Omega s(t) [(-I \cos(\delta\omega t) + Q \sin(\delta\omega t)) \sigma_x + (I \sin(\delta\omega t) + Q \cos(\delta\omega t)) \sigma_y], \quad (33)$$

where $\delta\omega = \omega_{01} - \omega_d$ and the “fast” $\omega_{01} + \omega_d$ terms have being ignored. After some trigonometric manipulation (as in lectures & problem sets):

$$\tilde{H}_d = -\frac{\Omega}{2} s(t) \begin{pmatrix} 0 & e^{j(\delta\omega t + \phi)} \\ e^{-j(\delta\omega t + \phi)} & 0 \end{pmatrix}. \quad (34)$$

That way, assuming $\delta\omega = 0$:

$$\tilde{H}_d = -\frac{\Omega}{2} s(t) (I \sigma_x + Q \sigma_y). \quad (35)$$

In order to find the effect of the driving signal to the qubit's state, the evolution operator is used (rotating frame):

$$\hat{U}(t) = e^{-j\tilde{H}_d t/\hbar}, \quad (36)$$

Depending on ϕ , the effect of $\hat{U}(t)$ on a state, resembles the application of rotation matrices. For example, assuming $\phi = 0$, $\hat{U}(t)$ becomes:

$$\hat{U}(t) = e^{j\frac{\Omega}{2\hbar} s(t) I \sigma_x}. \quad (37)$$

Solving for the arbitrary state $|\psi(t)\rangle = \hat{U}(t) |\psi(0)\rangle$ (as per lectures), one can see that the envelope of the driving signal $s(t)$ directly controls the speed of rotation. Thus, to allow for precise control of the rotation angle, it is integrated over a specific time window. That way the rotation angle can be controlled by the area of the pulse $s(t)$. Thus, the evolution operator is written as:

$$\hat{U}_k(t_p) = e^{-\frac{j}{2\hbar} \Theta_k(t_p) (I_k \sigma_x + Q_k \sigma_y)}, \quad (38)$$

where $\Theta(t_p) = -j\Omega \int_0^{t_p} s(\tau) d\tau$. It can be seen that depending on the driving phase ϕ , the rotation axis is controlled, e.g., for $\phi = 0$, i.e., a pulse on the I component of the quadrature signal, the state will rotate around the x axis with an angle given by $\Theta(t_p)$. An example gate operation is depicted in Fig. 6. The phase ϕ of the driving signal, initially, has an arbitrary reference point. Given an initial operation/pulse, however, subsequent phases of the driving signal can be defined and an axis selection be performed. As an example, a rotation of ϕ_0 around the z -axis can be performed using subsequent pulses, that differ by ϕ_0 in the I/Q phase [7]:

$$X_{\phi_0}^\dagger X_{\theta} X_{\phi_0} = e^{-\frac{j}{2\hbar} \Theta(t_{\theta}) (\cos(\phi_0) \sigma_x + \sin(\phi_0) \sigma_y)} X_{\theta} = Z_{-\phi_0} X_{\theta} Z_{\phi_0} X_{\theta}, \quad (39)$$

where X_{θ} denotes a rotation of θ rads around the x axis. The final rotation around the z axis ($-\phi_0$), does not affect the measurement result (assuming measurement on the z axis).

For building fast gates, short pulses are required. But the shorter the pulses, the higher the bandwidth. Given the low anharmonicity offered by the transmon qubit, higher frequency content can lead to excitations to unwanted energy levels. Thus, pulse shaping shall be performed as a tradeoff between speed and correct operation (using, for example, Gaussian pulses, the DRAG scheme [1]).

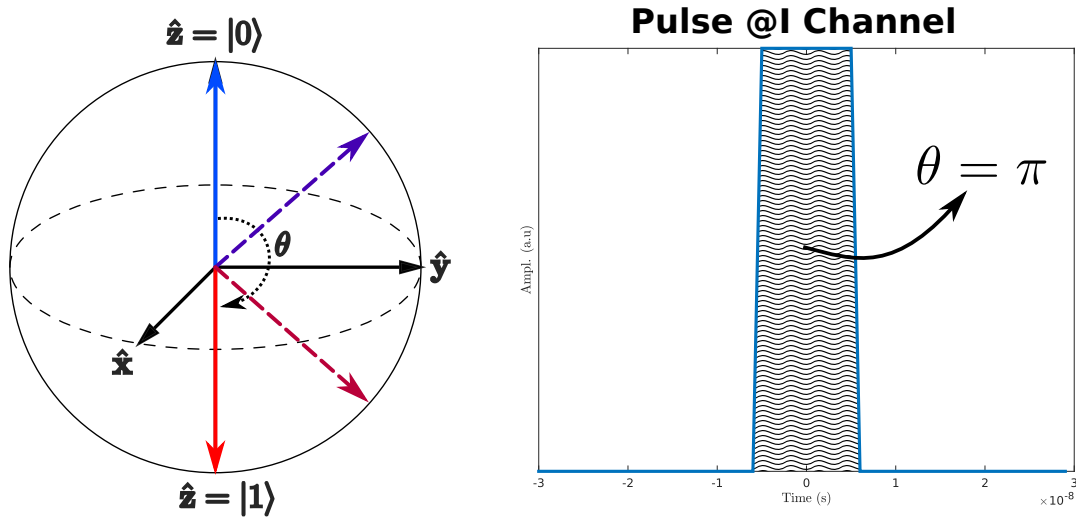


Fig. 6: A pulse of specific area (amplitude, duration) at the I channel ($\phi = 0$) corresponds to a rotation around x axis. In the example depicted, a pulse of $\theta = \pi$ with $\phi = 0$ corresponds to a NOT operation (up to a phase).

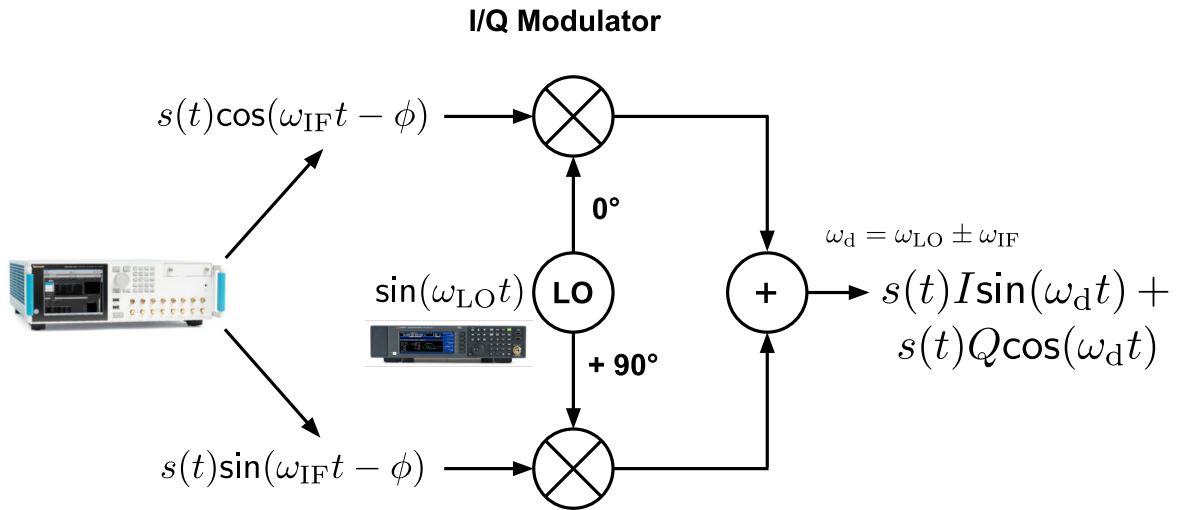


Fig. 7: Example of a setup used for generating the signals for controlling the state of a qubit

An example of a setup for generating the driving signals is depicted in Fig. 7. An arbitrary waveform generator (AWG) produces properly designed pulses $s(t)$ corresponding to a specific rotation angle. The signal produced by the AWG is at an intermediate frequency (IF) which is then upconverted using an I/Q modulator and an RF generator. The RF generator produces a carrier at ω_{LO} . Given the high values of ω_{01} , it is hard to find AWGs that can produce arbitrary waveforms centered at such frequencies. Another reason for the use of the mixing setup is that (as will be discussed in the next section), the AWG can synthesize multiple baseband signals at different ω_{IF} s and thus address multiple qubits.

V. TWO QUBIT GATES

A. Qubit Tuning

To implement multiple qubit gates, the involved qubits must be able to interact. At the same time, means of controlling the said interaction should be provided, so as to individually address each qubit when interaction is not required (in the case of single qubit gates). In the case of the superconducting

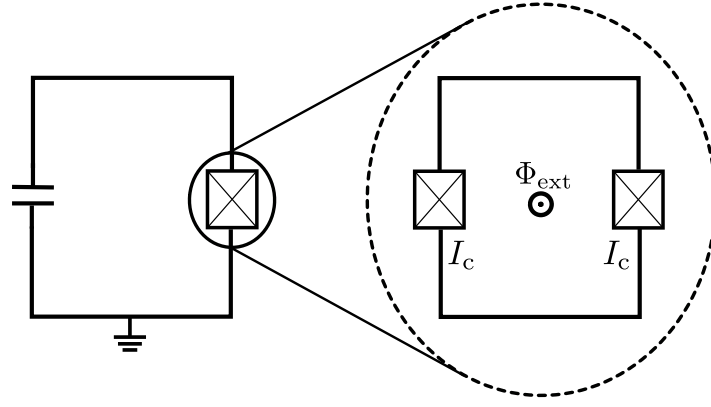


Fig. 8: Arrangement of a number of Josephson junctions so as to allow for resonance tuning. An externally applied magnetic flux Φ_{ext} controls E_J and by extension the qubit's resonance frequency.

qubit, the interaction between two qubits can be controlled by tuning the resonance frequency of the involved (in the interaction) qubit(s).

It can be seen from Eq. (25) that tuning the resonance frequency of a qubit, is a matter of adjusting either of E_c , E_J . Using a number of appropriately arranged Josephson junctions, E_J can be adjusted by means of an externally applied magnetic flux [1]. An arrangement allowing for controlling the resonance of the qubit by an externally applied flux Φ_{ext} , is shown in Fig. 8. Based on the arrangement of Fig. 8, the Hamiltonian of the system can be expressed as [1]:

$$\hat{H} = 4E_c\hat{n}^2 - 2E_J|\cos(\phi_e)|\cos(\hat{\phi}) = 4E_c\hat{n}^2 - E'_J(\phi_e)\cos(\hat{\phi}), \quad (40)$$

where $\phi_e = \pi\Phi_{\text{ext}}/\Phi_0$. Using $E'_J(\phi_e) = 2E_J|\cos(\phi_e)|$ and Eq. (25), the resonance frequency of a system described by Eq. (40), is shown in Fig. 9. The sensitivity of the system's resonance frequency to the external field is evident. Small variations in the applied magnetic field (flux noise) can result in significant detuning of the qubit. There exist architectures (e.g., by utilizing assymmetric Josephson junctions or using chains of junctions) that can minimise the sensitivity of the resonance frequency to flux noise, while providing sufficient tuning range [1].

B. Capacitively Coupled Qubits & the SWAP Gate

Tuning a first qubit to the resonance frequency of a second qubit (as described in Sec. V-A) so that interaction can occur, assumes that the said qubits are somehow coupled together. A method for "connecting" those qubits together, is to couple them using a capacitor (see Fig. 10).

Similarly to Sec. IV, the Hamiltonian of the system depicted in Fig. 10 is given by :

$$\hat{H} = \hat{H}_1 + \hat{H}_2 + C_g V_1 V_2, \quad (41)$$

where \hat{H}_1 , \hat{H}_2 give the Hamiltonian for each of the individual qubits and $\hat{H}_{\text{qq}} = C_g V_1 V_2$ is the Hamiltonian describing the interaction. By assuming a system limited to the two lowest energy levels, similarly to Sec. IV, the Hamiltonian of Eq. (41) becomes:⁵

$$\hat{H} = -\frac{1}{2}\hbar\omega_{q,1}\sigma_{z,1} - \frac{1}{2}\hbar\omega_{q,2}\sigma_{z,2} + g\sigma_{y1}\sigma_{y2}, \quad (42)$$

where g is a factor accounting for the coupling strength. g depends on the resonance frequency of each qubit and on the involved capacitances. Utilizing σ^\pm operators while employing the rotating wave approximation (higher frequency terms are omitted), the interaction Hamiltonian can be expressed as:

$$\hat{H}_{\text{qq}} = g(e^{j\delta\omega_{12}t}\sigma^+\sigma^- + e^{-j\delta\omega_{12}t}\sigma^-\sigma^+), \quad (43)$$

⁵It is also assumed that $C_g \ll C_{1,2}$.

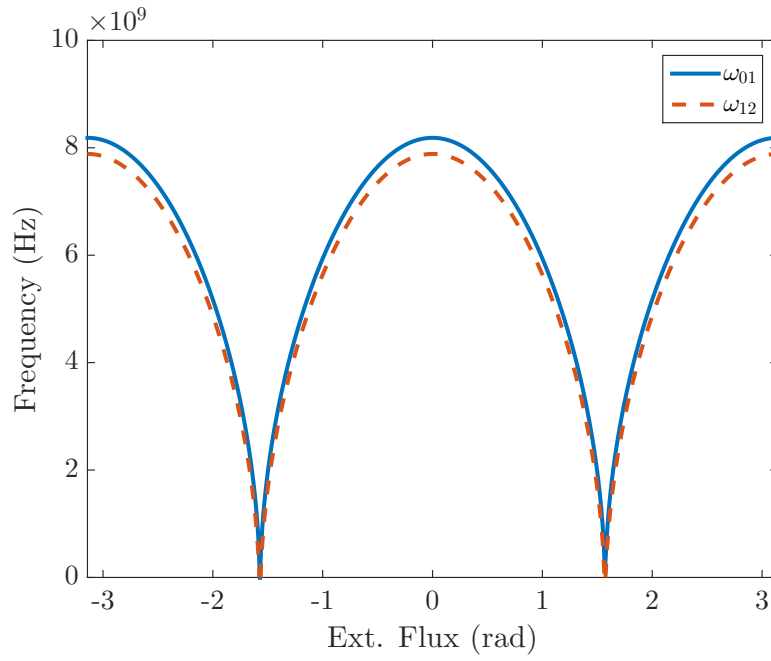


Fig. 9: An external magnetic field Φ_{ext} is used to tune the resonance frequency of the qubit. The behaviour depicted in the plot corresponds to the architecture of Fig. 8.

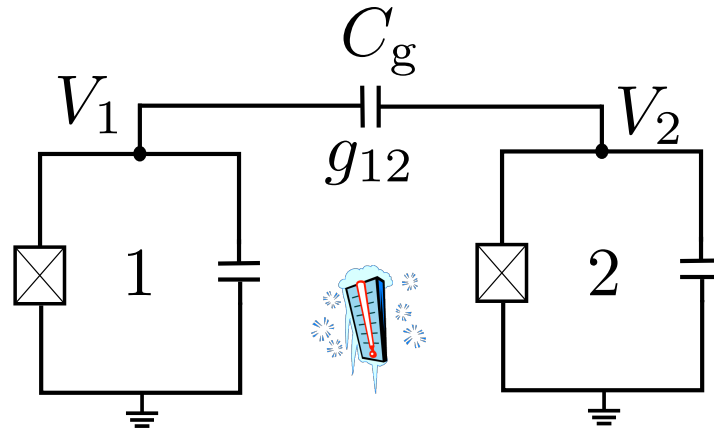


Fig. 10: Capacitive coupling of two qubits allowing for their interaction. Interaction can be controlled by bringing, for example, qubit #1 “in resonance” with qubit #2.

where $\delta\omega_{12} = \omega_{q,1} - \omega_{q,2}$. Given $\delta\omega_{12} = 0$, Eq. (43) shows that there is a constant exchange of excitations between the two qubits. For example, when qubit #1 “drops” from its excited state to its ground state, a photon of energy $\hbar\omega_{q,1}$ is emitted. Assuming qubit #2 is in its ground state, given sufficient coupling and the fact that $\delta\omega_{12} = 0$, the former will absorb the emitted (from #1) photon and as a result, it will be excited to its higher energy state. This exchange of excitations will continue for as long the two qubits are in resonance ($\delta\omega_{12} = 0$).

The aforementioned interaction (constant exchange of excitations) constitutes a SWAP gate. Assuming $\delta\omega_{12} = 0$, the interaction Hamiltonian can be rewritten as:

$$\hat{H}_{\text{qq}} = g (\sigma^+ \sigma^- + \sigma^- \sigma^+) = \frac{g}{2} (\sigma_x \sigma_x + \sigma_y \sigma_y). \quad (44)$$

Thus, the unitary operator corresponding to the interaction described by the above equation is given by:

$$U_{\text{qq}}(t) = e^{-j\frac{g}{2}(\sigma_x\sigma_x + \sigma_y\sigma_y)t} = \begin{bmatrix} 1 & 0 & 0 & 0 \\ 0 & \cos(gt) & -j\sin(gt) & 0 \\ 0 & -j\sin(gt) & \cos(gt) & 0 \\ 0 & 0 & 0 & 1 \end{bmatrix}. \quad (45)$$

Bringing the qubits in resonance for a specific time of $t_{\text{sw}} = \frac{\pi}{2g}$ results in:

$$U_{\text{qq}}\left(\frac{\pi}{2g}\right) = \begin{bmatrix} 1 & 0 & 0 & 0 \\ 0 & 0 & -j & 0 \\ 0 & -j & 0 & 0 \\ 0 & 0 & 0 & 1 \end{bmatrix} = j\text{SWAP}. \quad (46)$$

The j in front of the SWAP gate accounts for the phase term $e^{j\frac{\pi}{2}}$. “Looking” in the evolution at different time instants, will “find” the system at different states. For example, superposition of $|01\rangle$, $|10\rangle$ (up to a phase) occurs (periodically) at time instant $t_{\text{sp}} = \frac{\pi}{4g}$.

C. The CPHASE Gate

The CPHASE gate applies a phase ($e^{j\pi}$) to the qubits when they are excited at $|11\rangle$. Such operation occurs naturally in transmon qubits when exploiting interaction of $|11\rangle$ with higher (outside of the computational space) energy states.

The spectrum of energy levels in a transmon qubit,⁶ exhibits a characteristic frequency splitting between the energy levels of (computational) state $|11\rangle$ and (non-computational) energy state $|20\rangle$. The splitting (in the order of 10s of MHz), allows for phase accumulation of π rads. The characteristic phase accumulation only occurs at the interaction point of $|11\rangle$ and $|20\rangle$, thus the CPHASE is effectively realized.

In Sec. V-B, it was assumed that the a qubit is detuned so as to be brought in resonance with a second qubit. Looking into a qubit’s Hamiltonian in the computational space (Eq. (29)), it can be seen that detuning the qubit results in an accumulation of phase:

$$\theta_{z,1} = \int_0^{\tau_{\text{det}}} \omega_{q,1} - \omega(t) dt, \quad (47)$$

where τ_{det} is the period for which detuning occurs and $\omega(t)$ is the detuning. Thus, during the tuning required for getting to the $|11\rangle$, $|20\rangle$ characteristic splitting, besides the desired phase of π , phase is also introduced due to the detuning of the qubit from its initial resonance point. Given knowledge of the detuning “path” ($\omega(t)$), the unwanted detuning phase can be removed via a Z operation. It must be mentioned that the tuning path should be chosen carefully so as to avoid crossing to the $|20\rangle$ state. For an illustration of the procedure, kindly see Fig. 16 in [1], Fig. 2 in [8], Fig. 2 in [9] or attached presentation.

VI. MEASUREMENT

In order for state measurement to be performed, a qubit is considered “coupled” to a resonator (Fig. 11). Assuming resonance at its fundamental frequency ω_r , the resonator can be mathematically described as a quantum LC oscillator with the Hamiltonian and the associated energy eigenvalues given by Eq. (11) and Eq. (15), respectively.

When the resonator is “in tune” with the qubit, i.e., when $\omega_r \approx \omega_{01}$, there is a constant exchange of excitations (between the resonator and the qubit). When the resonator emits a photon by “falling” from an excited state, the qubit is excited to its high energy state by absorbing the said photon and vice versa. The exchange of excitations happens for as long as the resonator and the qubit are tuned.

⁶Considering tuning of the first qubit for the acquiring the spectrum.

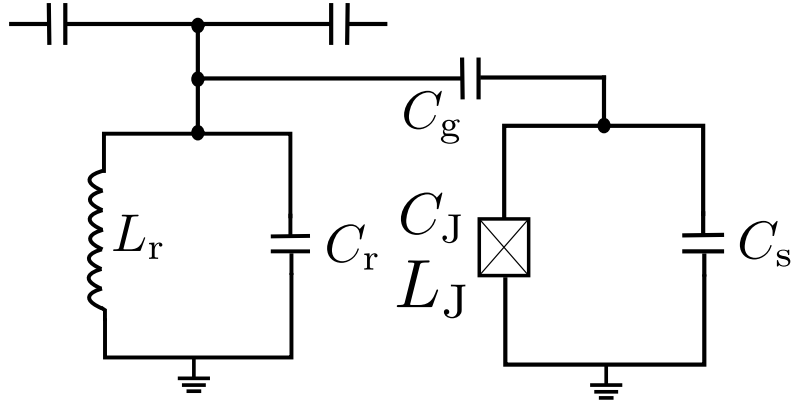


Fig. 11: Qubit state readout using a resonator. The resonator’s response to a driving signal is qubit-state dependent.

The aforementioned excitation loop occurs when the resonator is sufficiently coupled to the qubit, i.e., when $|\omega_r - \omega_{01}| \ll g$, where g is the coupling strength parameter. While in the case of multi-qubit interaction (see Sec. V) coupling is of essence, it is evident that in the case of state measurement is not acceptable.

When $\Delta = |\omega_r - \omega_{01}| \gg g$, the system is said to be in the “dispersive” regime. In that case, when driving the resonator (with a signal) at its (fundamental) resonance frequency, the presence of the qubit can be considered a perturbation on the resonator’s response. The same holds from the qubit’s perspective: the resonator’s driving signal is seen by the qubit as a perturbation to its dynamics. That way, it can be shown that the Hamiltonian of the resonator-qubit system can be expressed as [1]:

$$\hat{H}_{\text{rq}} = \hbar(\omega_r + \chi\sigma_z) \left(\hat{N}_r + 1/2 \right) + \frac{1}{2} \hbar \tilde{\omega}_{01} \sigma_z. \quad (48)$$

The term in front of $\left(\hat{N}_r + 1/2 \right)$ defines the resonator’s resonance frequency (see Sec II). As it can be seen from Eq. (48), the resonator’s resonance is shifted by $\pm\chi = g^2/\Delta$ depending on the qubit’s state (σ_z operator). Depending on the state, the fundamental of the resonator will either be $\omega_r^{(0)} = \omega_r + \chi$ or $\omega_r^{(1)} = \omega_r - \chi$. Thus, the qubit can be probed so as to measure its state, by examining the resonance frequency of the resonator. As stated earlier the presence of the resonator affects the qubit’s dynamics as well. That is why $\tilde{\omega}_{01}$ is used instead of ω_{01} .

By driving the resonator with signals of different frequencies and measuring (at each of those frequencies), either the transmission (i.e., the characteristics of the signal at the “output” of the resonator, w.r.t. the input) or the reflection (i.e., the characteristics of the signal that is reflected back to the source), the state of the qubit can be inferred.

In practice, an RF signal at ω_{RO} is used to probe the resonator. Then, the amplitude and phase of the reflected (or transmitted) signal is measured. For the reasons described above, the values of those variables will depend on the qubit’s state. It has to be noted that choosing $\omega_{\text{RO}} = \omega_r^{(0)} + \omega_r^{(1)}$, leads to maximal discrimination between the values of the variables that are measured to infer the qubit’s state; choosing the aforementioned value for ω_{RO} , leads to a constant amplitude but maximal separation of the phase component of the reflected (or transmitted) signal [1].

REFERENCES

- [1] P. Krantz, M. Kjaergaard, F. Yan, T. P. Orlando, S. Gustavsson, and W. D. Oliver, “A quantum engineers guide to superconducting qubits,” *Applied Physics Reviews*, vol. 6, no. 2, p. 021318, Jun. 2019.
- [2] L. Susskind and A. Friedman, *Quantum Mechanics: The Theoretical Minimum*. Penguin Books, 2015.
- [3] N. K. Langford, “Circuit QED - Lecture Notes,” 2019. [Online]. Available: <http://arxiv.org/abs/1905.05130>
- [4] R. P. Feynman, *The Feynman Lectures on Physics*, vol. 3. [Online]. Available: <https://www.feynmanlectures.caltech.edu/>

- [5] J. M. Fink, “Quantum Nonlinearities in Strong Coupling Circuit QED,” Ph.D. dissertation, ETH Zurich, 2017.
- [6] J. Koch *et al.*, “Charge-insensitive qubit design derived from the Cooper pair box,” *Physical Review A*, vol. 76, no. 4, Oct. 2007.
- [7] D. C. McKay *et al.*, “Efficient Z gates for quantum computing,” *Physical Review A*, vol. 96, no. 2, Aug. 2017.
- [8] L. DiCarlo *et al.*, “Demonstration of two-qubit algorithms with a superconducting quantum processor,” *Nature*, vol. 460, no. 7252, p. 240244, Jun. 2009.
- [9] —, “Preparation and measurement of three-qubit entanglement in a superconducting circuit,” *Nature*, vol. 467, no. 7315, p. 574578, Sep. 2010.